Journal of Hazardous Materials B118 (2005) 155–160

Journal of Hazardous Materials

www.elsevier.com/locate/jhazmat

Photooxidative degradation of Acid Red 27 in a tubular continuous-flow photoreactor: influence of operational parameters and mineralization products

N. Daneshvar[b,*], M. Rabbani[a], N. Modirshahla[c], M.A. Behnajady[a]

[a] *Department of Applied Chemistry, Faculty of Chemistry, Islamic Azad University, North Tehran Branch, P.O. Box 19585/936, Tehran, Islamic Republic of Iran*

[b] *Water and Wastewater Treatment Research Laboratory, Department of Applied Chemistry, Faculty of Chemistry, University of Tabriz, C.P. 51664, Tabriz, Islamic Republic of Iran*

[c] *Research Laboratory, Department of Applied Chemistry, Islamic Azad University, Tabriz Branch, P.O. Box 1655, Tabriz, Islamic Republic of Iran*

Received 4 July 2004; received in revised form 14 October 2004; accepted 16 October 2004
Available online 8 December 2004

Abstract

The decolorization and mineralization of Acid Red 27 (AR27), an anionic monoazo dye of acid class, was investigated using UV radiation in the presence of H_2O_2 in a tubular continuous-flow photoreactor as a function of oxidant concentration, reactor length, flow rate and light intensity. The removal efficiency of AR27 depends on the operational parameters and increases as the initial concentration of H_2O_2 and light intensity are increased but it decreases when the flow rate is increased. The AR27 degradation was followed through HPLC, UV–vis and COD analyses. The results of these analyses showed that the final outlet stream from the photoreactor was completely mineralized. The UV/H_2O_2 process was also able to mineralize nitrogen and sulfur heteroatoms into NH_4^+, NO_3^-, NO_2^- and SO_4^{2-} ions, respectively. The nitrogen of azo group was transformed predominantly to NH_4^+ ions. Decreasing the flow rate results in the reduction of COD and promotion of SO_4^{2-} at the final outlet stream of the photoreactor.

Keywords: Advanced oxidation processes (AOPs); Decolorization; Mineralization; Continuous photoreactor; Acid Red 27

1. Introduction

Dye pollutants from textile industry are an important source of environmental contamination. It is estimated that 1–15% of the dye is lost during dyeing and finishing processes and is released in wastewaters [1]. The release of these colored wastewaters poses a major problem for the industry as well as a threat to the environment [2]. Among the 10 000 different dyes and pigments available, azo dyes constitute over 50% of all textile dyes used in the industry [3]. Some of these dyes, are toxic and nonbiodegradable, therefore, cannot be treated efficiently using conventional treatment processes [4].

Advanced oxidation processes (AOPs) provide a promising technique for treatment of textile industry wastewater [5–11]. Homogenous advanced oxidation process employing hydrogen peroxide with UV light has been found to be very effective in the degradation of dyes [12,13]. This process involves the production of hydroxyl radicals ($^{\bullet}OH$) that are extremely reactive and strong oxidizing agent ($E^0 = 2.8$ V) capable of mineralizing organic contaminants. Reaction of hydroxyl radicals generated in the presence of an organic substrate may occur via one of the three general pathways: (1) hydrogen abstraction; (2) electrophilic addition and (3)

* Corresponding author. Tel.: +98 411 5255825/3393146; fax: +98 411 3340191.
E-mail address: nezam_daneshvar@yahoo.com (N. Daneshvar).

0304-3894/$ – see front matter © 2004 Elsevier B.V. All rights reserved.
doi:10.1016/j.jhazmat.2004.10.007

electron transfer [10]. The UV/H_2O_2 process in comparison to other methods of water treatment has additional advantages such as no formation of sludge during the treatment and high removal rates of chemical oxygen demand (COD) [14].

Many studies used bath photoreactor, which was irradiated by a UV lamp from above the solution or immersion lamps [5–9]. In our previous work, we reported the effect of operational parameters on photooxidative degradation of Acid Red 27 (AR27) by UV/H_2O_2 process in a batch photoreactor [12], so the aim of the present work is the photooxidative degradation of higher concentration of AR27 in a tubular continuous-flow photoreactor and examination of the effect of operational parameters, such as oxidant concentration, reactor length, flow rate and light intensity, at decolorization and degradation of this dye. Finally, to follow the mineralization of AR27 in this photoreactor HPLC chromatograms, UV–vis spectra, inorganic ions evolution and COD reduction were recorded at different lengths of photoreactor.

2. Experimental

2.1. Materials

Acid Red 27, a monoazo anionic dye, was obtained from Boyakh Saz Company (Iran). Its chemical structure is given in Fig. 1. The hydrogen peroxide solution (30%) was purchased from Merck (Germany). Solutions were prepared by dissolving the requisite quantity of the dye in double distilled water.

2.2. Photoreactor

All experiments were carried out in a tubular continuous-flow photoreactor. A schematic diagram has been shown in Fig. 2. The photoreactor comprises four quartz tubes (24.4 mm i.d., 26 mm o.d., 87 cm long), which were serially connected by means of transparent rubber tubes from the top to the bottom. The radiation source consists of four mercury UV lamps (30 W, UV-C, manufactured by Philips, Holland) in vertical arrays, which were placed in front of the quartz tubes. The distance between the lamps and the quartz tubes

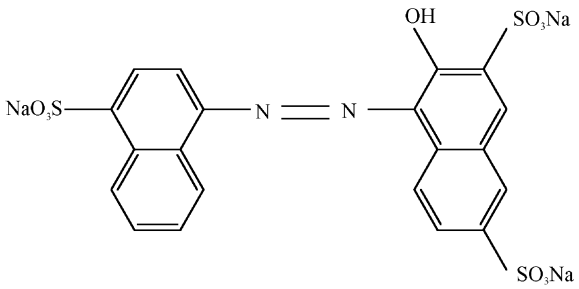

Fig. 1. Chemical structure of AR27 (C.I. 16185).

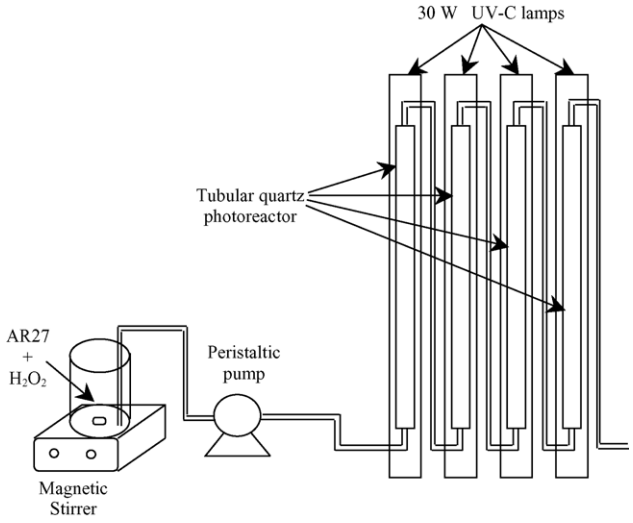

Fig. 2. Schematic diagram of tubular continuous-flow photoreactor. For details refer to text.

was 5 cm and variation in the distance caused the change of the light intensity.

2.3. Procedures

For photooxidative degradation of AR27, a solution containing known concentrations of dye and H_2O_2 was prepared and then 2 l of the prepared solution was transferred into a Pyrex beaker and agitated with a magnetic stirrer during experiment. The solution was pumped with a peristaltic pump through the irradiated quartz tubes and AR27 concentration at the inlet and outlet was analyzed with a UV–vis spectrophotometer (Ultrospec 2000, Biotech Pharmacia, England) at 521 and 254 nm. The absorbance at 521 nm is due to the color of the dye solution and it is used to monitor the decolorization of the dye. The absorbance at 254 nm represents the aromatic content of AR27 and absorbance decrease at 254 nm indicates the degradation of aromatic part of the dye [14]. The changes in the absorption spectra of AR27 at different lengths of photoreactor were recorded on a double-beam UV–vis spectrophotometer (Shimadzu 1700) in the wavelength range from 190–700 nm.

Chemical oxygen demand was measured by the dichromate reflux method [15]. The formation of SO_4^{2-}, NH_4^+, NO_3^- and NO_2^- ions was determined by turbidimetric, direct nesslerization and manual cadmium reduction methods, respectively [16].

High-performance liquid chromatograms were recorded on an HPLC (Perkin-Elmer Series 200). A Spheri-5 RP-18 column with dimension of 220 mm × 4.6 mm and with 5-μm particle size and UV–vis detector with the wavelength set at 254 nm were used. The mobile phase was a mixture of acetonitrile–water 30/70 (v/v) at a flow rate of 0.9 ml min^{-1}.

The light intensity in the center of the photoreactor was measured by a Lux-UV-IR meter (Leybold Co.).

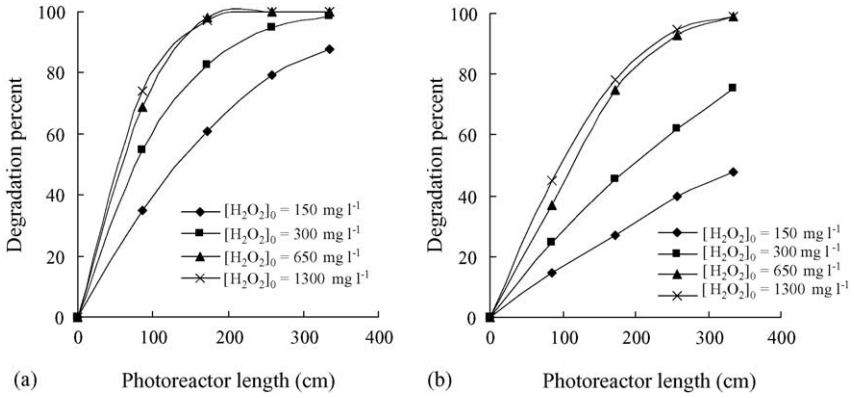

Fig. 3. Effect of the initial concentration of H_2O_2 at decolorization (a) and degradation (b) of AR27. $[AR27]_0 = 150\,mg\,l^{-1}$, flow rate = 43 ml min^{-1}, $I_0 = 43\,W\,m^{-2}$.

3. Results and discussion

3.1. Influence of operational parameters at decolorization and degradation of AR27

3.1.1. Effect of the initial concentration of H_2O_2

The decolorization and degradation efficiency versus photoreactor length at different initial concentrations of H_2O_2 (150–1300 $mg\,l^{-1}$) have been summarized in Fig. 3a and b, respectively. The decolorization and degradation efficiency increases with increasing H_2O_2 concentration from 150 to 650 mg^{-1}. The enhancement of decolorization and degradation of AR27 in this course is due to an increase in the hydroxyl radical concentration. Further increase in H_2O_2 concentration resulted in only slight acceleration of the decolorization and degradation rate. At high H_2O_2 concentration, hydroxyl radical efficiently reacts with H_2O_2 and produces $HO_2^{\bullet}$ (Eq. (1)), also $^{\bullet}OH$ radicals generated at high concentration react with $HO_2^{\bullet}$ (Eq. (2)) or dimerize to H_2O_2 (Eq. (3)). It is obvious that $HO_2^{\bullet}$ radicals are less reactive than $^{\bullet}OH$ radicals, therefore leading to negligible contribution in the dye removal [17,18].

$$H_2O_2 + {}^{\bullet}OH \xrightarrow{k_1} HO_2^{\bullet} + H_2O \quad (1)$$

$k_1 = 2.7 \times 10^7\,M^{-1}\,s^{-1}$ [17],

$$^{\bullet}OH + HO_2^{\bullet} \xrightarrow{k_2} H_2O + O_2 \quad (2)$$

$k_2 = 6.6 \times 10^9\,M^{-1}\,s^{-1}$ [18],

$$^{\bullet}OH + {}^{\bullet}OH \xrightarrow{k_3} H_2O_2 \quad (3)$$

$k_3 = 5.5 \times 10^9\,M^{-1}\,s^{-1}$ [17].

Fig. 3a shows decolorization of AR27 (150 $mg\,l^{-1}$) in the presence of 650 $mg\,l^{-1}$ of H_2O_2 completed in 200 cm from photoreactor length, but as shown in Fig. 3b for complete degradation of AR27 photoreactor length must be around 340 cm.

3.1.2. Effect of the flow rate

The decolorization and degradation efficiency versus photoreactor length at different flow rates have been summarized

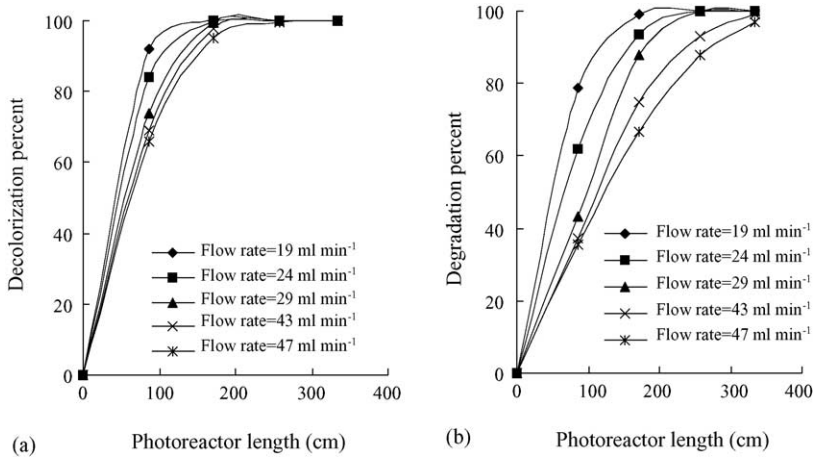

Fig. 4. Effect of the flow rate at decolorization (a) and degradation (b) of AR27. $[AR27]_0 = 150\,mg\,l^{-1}$, $[H_2O_2]_0 = 650\,mg\,l^{-1}$, $I_0 = 43\,W\,m^{-2}$.

in Fig. 4a and b, respectively. The results indicate that with decreasing flow rate from 47 to 19 ml min^{-1}, removal efficiency is increased, so that the complete decolorization and degradation were obtained at around 100 and 180 cm from photoreactor length, respectively. This is logical, because with decreasing flow rate the residence time of the reactant increases in the reactor.

3.1.3. Effect of the light intensity

The effect of the light intensity at the decolorization and degradation of AR27 was shown in Fig. 5. The results show that the removal percent steadily increased with increasing the light intensity linearly. The increase in the light intensity from 13.55 to 58.5 W m^{-2} increases the decolorization from 16.8 to 81% and degradation from 7.9 to 46.5% for 86 cm of photoreactor length (first outlet from photoreactor). The results show that the UV light intensity plays an important role in degradation of AR27. This is due to effective role of light intensity in the formation of high amounts of $^{\bullet}OH$ from H_2O_2 in the solution, which can be used for decolorization and degradation of AR27 (Eq. (4)). The linear relation between removal percent and light intensity shows that UV light intensity used in this work is in the low region [14].

$$H_2O_2 + h\upsilon \xrightarrow{k_4} 2^{\bullet}OH \quad (4)$$

3.2. Mineralization and final products of degradation of AR27

Mineralization of AR27 in UV/H_2O_2 process at different lengths of photoreactor was studied with a 150 mg l^{-1} AR27 solution in the presence of 650 mg l^{-1} hydrogen peroxide. Mineralization was studied by COD loss, changes in HPLC chromatograms and UV–vis spectra and also SO_4^{2-}, NH_4^+, NO_3^- and NO_2^- evolution at different lengths of photoreactor.

COD values have been related to the total concentration of organics in the solution and the decrease of COD reflects the degree of mineralization as a function of photoreactor length. Fig. 6 shows the decrease of COD versus photoreactor length at two different flow rates. Results indicate that the

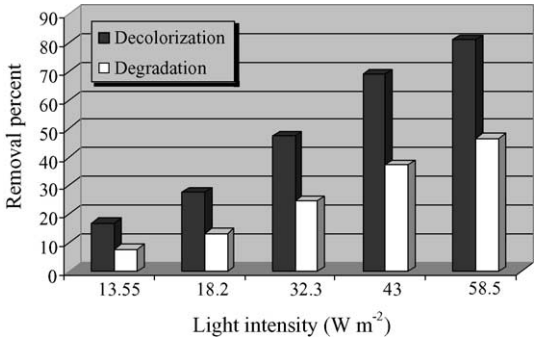

Fig. 5. Effect of the light intensity at decolorization and degradation of AR27. $[AR27]_0 = 150$ mg l^{-1}, $[H_2O_2]_0 = 650$ mg l^{-1}, flow rate = 43 ml min^{-1}, photoreactor length = 86 cm.

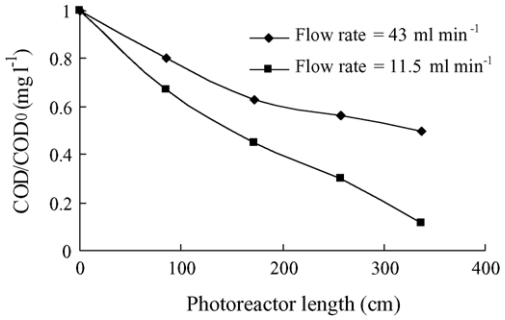

Fig. 6. COD changes versus photoreactor length at two different flow rates. $[AR27]_0 = 150$ mg l^{-1}, $[H_2O_2]_0 = 650$ mg l^{-1}, $I_0 = 58$ W m^{-2}.

amount of COD declined with photoreactor length but final COD at flow rate of 43 ml min^{-1} is fairly high. For decreasing final COD in outlet stream of the photoreactor, flow rate was dropped to 11.5 ml min^{-1}. In this flow rate, final COD value in outlet stream from photoreactor is very low. This results show complete mineralization can be obtained in fairly low flow rates.

The evolution of SO_4^{2-} ions is presented in Fig. 7 for two different flow rates. According to the AR27 molecular structure in Fig. 1 the three sulfonic groups connected with the two kinds of naphthalene rings. Fig. 7 shows the initial slope at both flow rates is positive, indicating that SO_4^{2-} ions are initial products, directly resulting from the initial attack on the sulfonic groups. Some other SO_4^{2-} ions can be evolved from the degradation of intermediates—SO_3^-. The release of SO_4^{2-} ions could be due to an initial attack by $^{\bullet}OH$ radicals.

$$R\text{–}SO_3^- + {}^{\bullet}OH \rightarrow R\text{–}OH + SO_3^{\bullet -} \quad (5)$$

$$SO_3^{\bullet -} + OH^- \rightarrow SO_4^{2-} + H^{\bullet} \quad (6)$$

The hydrogen atom $H^{\bullet}$ can subsequently react with hydroxyl radicals [19]:

$$^{\bullet}OH + H^{\bullet} \rightarrow H_2O \quad (7)$$

Results in Fig. 7 show that final quantity of SO_4^{2-} at flow rate of 44 ml min^{-1} is 25.6 mg l^{-1}, whereas its amount at the end of the photoreactor can be reached to 37.27 mg l^{-1} with decreasing flow rate to 11.5 ml min^{-1}. The final concentra-

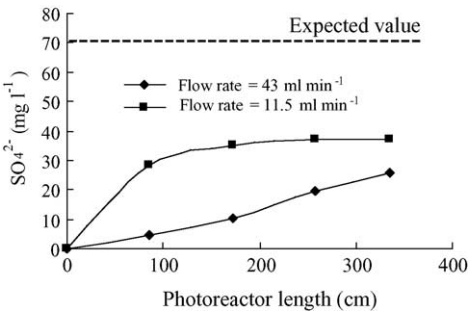

Fig. 7. SO_4^{2-} evolution versus photoreactor length at two different flow rates. $[AR27]_0 = 150$ mg l^{-1}, $[H_2O_2]_0 = 650$ mg l^{-1}, $I_0 = 58$ W m^{-2}.

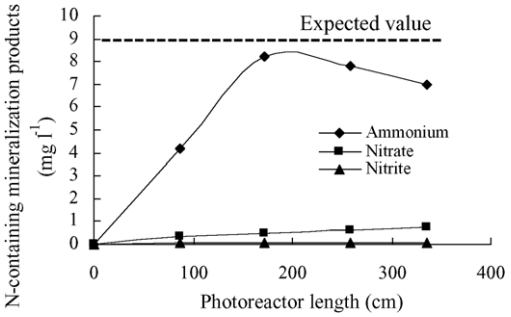

Fig. 8. N-containing mineralization products evolution versus photoreactor length. $[AR27]_0 = 150\,mg\,l^{-1}$, $[H_2O_2]_0 = 650\,mg\,l^{-1}$, flow rate = 43 ml min^{-1}, $I_0 = 58\,W\,m^{-2}$.

tion of SO_4^{2-} produced in outlet stream cannot reach to an expected value, which is in agreement with other findings. This could be explained by the formation of sulfur dioxide [20,21].

The evolution of NH_4^+, NO_3^- and NO_2^- as N-containing mineralization products versus photoreactor length are given in Fig. 8. The nitrogen mass balance, obtained with considering NH_4^+, NO_3^- and NO_2^- concentrations, almost corresponds to the final expected stoichiometric value at flow rate of 43 ml min^{-1}. As can be seen from Fig. 8, the main N-containing mineralization product of photooxidative degradation of AR27 is NH_4^+, and its value reaches to an expected value at 172 cm from photoreactor length. Decreasing the amount of NH_4^+ was observed in further photoreactor lengths. This is as a result of oxidation of NH_4^+ to NO_3^- and NO_2^- [22]. No significant NO_2^- ions were detected during the photooxidative degradation of AR27 at different lengths of photoreactor.

The changes in the UV–vis absorption spectra of AR27 solutions during the photooxidative degradation run at different photoreactor lengths have been shown in the Fig. 9. The decrease of the absorption peak of AR27 at λ = 521 nm in Fig. 9 indicates a rapid degradation of azo dye. The decrease is also meaningful with respect to the nitrogen-to-nitrogen double bond (–N=N–) of the azo dye, as the most active site for oxidative attack. As can be seen from Fig. 9a, final outlet stream from photoreactor is completely decolorized, but absorption spectrum in the UV-region was not disappeared. With decreasing the flow rate to 19 ml min^{-1} absorption spectrum in the UV-region for final outlet stream of the photoreactor is considerably reduced (Fig. 9b). Final absorption spectrum in UV-region can be related to the remained H_2O_2, which is used in high concentration and it has a strong absorption at this region. The absorption spectrum of H_2O_2 exhibits a slow and steady rise from 400 to 185 nm, and at 254 nm the molar absorptivity is about 19 l mol^{-1} cm^{-1} [23].

These results are in good agreement with HPLC chromatograms (Fig. 10). As can be seen from Fig. 10a, H_2O_2 only slightly was consumed throughout the decolorization

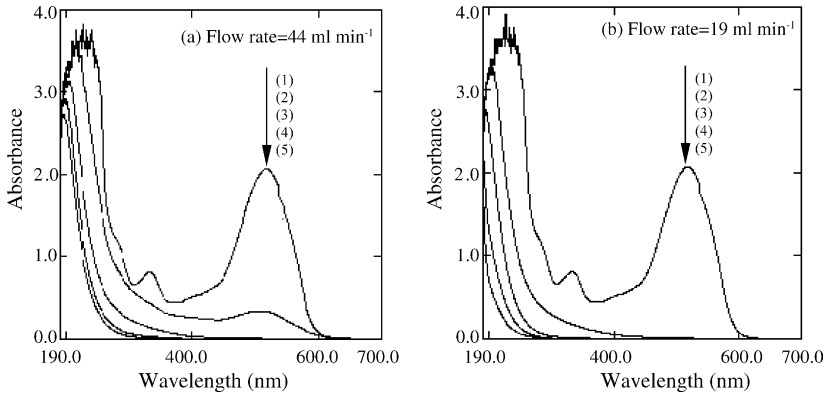

Fig. 9. UV–vis spectral changes of AR27, recorded during the dye degradation at different photoreactor lengths: (1) 0 cm, (2) 86 cm, (3) 172 cm, (4) 258 cm and (5) 335 cm. $[AR27]_0 = 150\,mg\,l^{-1}$, $[H_2O_2]_0 = 650\,mg\,l^{-1}$, $I_0 = 58\,W\,m^{-2}$.

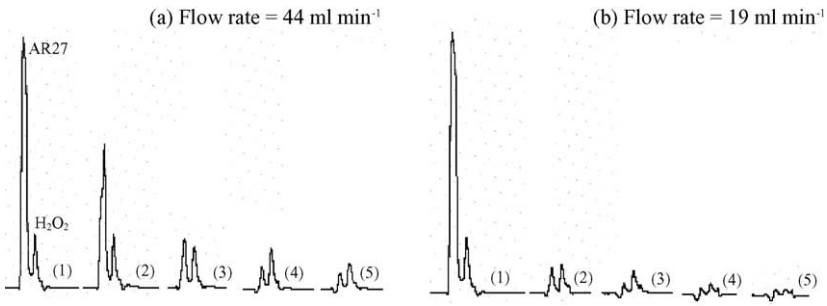

Fig. 10. HPLC chromatograms of the AR27, recorded during the dye degradation at different photoreactor lengths. (1) 0 cm, (2) 86 cm, (3) 172 cm, (4) 258 cm and (5) 335 cm. $[AR27]_0 = 150\,mg\,l^{-1}$, $[H_2O_2]_0 = 650\,mg\,l^{-1}$, $I_0 = 58\,W\,m^{-2}$.

process. The catalytic behavior of H_2O_2 has been observed by other authors [24]. The results in Fig. 9b and Fig. 10b show that after complete decolorization of AR27, depletion in H_2O_2 concentration was accelerated. Fig. 10a and b reveal that complete mineralization of AR27 could be achieved when flow rate was below 19 ml min^{-1}.

4. Conclusions

UV/H_2O_2 process can be used for complete decolorization and mineralization of AR27 as a monoazo anionic dye from acid class at high concentration in a continuous-flow photoreactor. Removal efficiency of AR27 in this photoreactor increases with increasing H_2O_2 concentration and light intensity. With decreasing flow rate, final COD was very low, also HPLC chromatograms and UV–vis absorption peaks mainly disappeared. Final mineralization products were NH_4^+, NO_3^-, NO_2^- and SO_4^{2-} ions. The nitrogen of azo group was transformed predominantly to NH_4^+ ions. With decreasing the flow rate from 44 to 11.5 ml min^{-1}, finally produced SO_4^{2-} in outlet stream increases from 25.6 to 37.27 mg l^{-1} and final COD decreases to very low amounts. The final optimum operational parameters for complete decolorization and mineralization of AR27 (150 mg l^{-1}) in this photoreactor are as follows: $[H_2O_2]_0 = 650$ mg l^{-1}, $I_0 = 58$ W m^{-2} and flow rate = 19 ml min^{-1}.

Acknowledgements

The authors thank the Islamic Azad University of North Tehran and Tabriz branches for financial and other supports, and also many thanks to Mrs. Skandari for HPLC chromatograms.

References

[1] T. Sauer, G.C. Neto, H.J. Jose, R.F.P.M. Moreira, J. Photochem. Photobiol. A 149 (2002) 147–154.
[2] M. Saquib, M. Muneer, Dyes Pigments 56 (2003) 37–49.
[3] Kirk-Othmer, Encyclopedia of chemical technology, third ed., John Wiley & Sons, 1978, pp. 387–433.
[4] H.L. Sheng, M.L. Chi, Water Res. 27 (1993) 1743–1748.
[5] N. Daneshvar, D. Salari, M.A. Behnajady, Iran. J. Chem. Chem. Eng. 21 (2002) 55–62.
[6] N. Daneshvar, D. Salari, A.R. Khataee, J. Photochem. Photobiol. A 157 (2003) 111–116.
[7] N. Daneshvar, D. Salari, A.R. Khataee, J. Photochem. Photobiol. A 162 (2004) 317–322.
[8] N. Daneshvar, M. Rabbani, N. Modirshahla, M.A. Behnajady, Chemosphere 56 (2004) 895–900.
[9] N. Daneshvar, M. Rabbani, N. Modirshahla, M.A. Behnajady, J. Photochem. Photobiol. A 168 (2004) 39–45.
[10] O. Legrini, E. Oliveros, A.M. Braun, Chem. Rev. 93 (1993) 671–698.
[11] I.K. Konstantinou, T.A. Albanis, Appl. Catal. B 49 (2004) 1–14.
[12] N. Daneshvar, M. Rabbani, N. Modirshahla, M.A. Behnajady, J. Environ. Sci. Health A 39 (2004) 2319–2332.
[13] M.A. Behnajady, N. Modirshahla, M. Shokri, Chemosphere 55 (2004) 129–134.
[14] M. Muruganandham, M. Swaminathan, Dyes Pigments 62 (2004) 271–277.
[15] APHA/AWWA/WPCF, Standards Methods for the Examination of Water and Wastewater, 17th ed., American Public Health Association, Washington, DC, 1989.
[16] ASTM, Annual Book of ASTM Standards, Water and Environmental Technology, vol. 11.01, ASTM International, Philadelphia, PA, 2000.
[17] G.V. Buxton, C.L. Greenstock, W.P. Helman, A.B. Ross, J. Phys. Chem. Ref. Data 17 (1988) 513–886.
[18] K. Schested, O.L. Rasmussen, H. Fricke, J. Phys. Chem. 72 (1968) 626–631.
[19] H. Lachheb, E. Puzenat, A. Houas, M. Ksibi, E. Elaloui, C. Guillard, J.M. Herrmann, Appl. Catal. B 39 (2002) 75–90.
[20] V. Brezova, M. Jankovicova, M. Soldan, A. Blazkova, M. Rehakova, I. Surina, M. Ceppan, B. Havlinova, J. Photochem. Photobiol. A 83 (1994) 69–75.
[21] E. Vulliet, C. Emmelin, J.M. Chovelon, C. Guillard, J.M. Herrmann, Environ. Chem. Lett. 1 (2003) 62–67.
[22] H. Chun, W. Yizhong, T. Hongxiao, Appl. Catal. B 35 (2001) 95–105.
[23] I. Nicole, J. De Laat, M. Dore, J.P. Duguet, C. Bonnel, Water Res. 24 (1990) 157–168.
[24] E.M. Elkanzi, G.B. Kheng, J. Hazard. Mater. B 73 (2000) 55–62.